Preprints.org

Article

Not peer-reviewed version

Machine Learning-Based Self-Induced Scratch Intensity Detection for Prevention of Lichenification Using Multi-Channel Electromyogram Muscle Synergy

Muhammad Omar Cheema , Alina Akhlaq , Zia Mohy Ud Din , Abdullah Al Aishan , Hedi Ammar Guesmi * , Jahan Zeb Gul *

Posted Date: 15 April 2026

doi: 10.20944/preprints202604.1050.v1

Keywords: chronic pruritus; electromyography; scratching intensity detection; feature extraction; recursive feature elimination; biomedical signal classification

 doi:10.20944/preprints202604.1050.v1

Article

Machine Learning-Based Self-Induced Scratch Intensity Detection for Prevention of Lichenification Using Multi-Channel Electromyogram Muscle Synergy

Muhammad Omar Cheema [1], Alina Akhlaq [2], Zia Mohy Ud Din [1], Abdullah Al Aishan [3], Hedi Ammar Guesmi [4,*] and Jahan Zeb Gul [5,*]

[1] Air University
[2] HITEC University
[3] King Khalid University
[4] Qassim University
[5] Maynooth University
* Correspondence: h.guesmi@qu.edu.sa (H.A.G.); jahanzeb.gul@mu.ie (J.Z.G.)

Abstract

Chronic pruritus in patients with dermatological conditions causes physical discomfort, skin breakdown, sleep disturbance, and overall decline in quality of life. Persistent scratching can lead to a condition known as lichenification, which further deteriorates the skin. Lichenified skin is more susceptible to infections, which further complicates the treatment and prolongs the recovery time. This highlights the importance of accurately detecting and quantifying scratching behavior for effective management and intervention. All the existing technologies to monitor scratching involve the use of external sensor modalities such as an accelerometer and a gyroscope, followed by camera monitoring. However, such scratch detection methods are limited in their reliability in monitoring scratching intensity. This study aims to acquire muscle activity to accurately detect, quantify, and provide feedback on self-induced scratching intensity. Through a meticulous understanding of the synergies of hand muscles, three out of seven forearm muscles were identified that generate consistent and distinctive signals during scratching motion. These signals were acquired, preprocessed, segmented, and analyzed using both time and frequency domain features. The extracted 45 features of 3-Channel EMG signals were first optimized using recursive feature elimination and validated by cross-validation accuracies of the recursive feature elimination technique, with the highest optimized accuracy of 0.8628 when EMG of a complete combination of muscles is used. This study shows the promising results in facilitating enhanced diagnosis and management of scratching intensities. The model can be deployed into an embedded device for generating alerts and providing advanced therapy.

Keywords: chronic pruritus; electromyography; scratching intensity detection; feature extraction; recursive feature elimination; biomedical signal classification

1. Introduction

Itch or pruritus may be the result of many different factors, such as dermatological, neurological, and systemic diseases [1,2]. It is among the most irritating symptoms in patients, which appear due to allergic cutaneous illnesses like atopic dermatitis and eczema, infections, and an adverse drug reaction [3]. Itching has a serious negative impact on the quality of life, causing insomnia and even depression [3,4]. Research has shown that chronic pruritus (more than six weeks) has an incidence of approximately 10% of the world population, and 91% of victims of atopic dermatitis have the

doi:10.20944/preprints202604.1050.v1

condition [3–6]. The Centers for Disease Control and Prevention estimates 1.7 million skin infections are reported every year in the United States [8]. In 2023, recent statistics illustrate that there remains a health concern and that there have been recent spikes to 5.8 million new cases annually [7]. This growth highlights the importance of the need to develop powerful monitoring and prevention systems.

In the clinical picture, itch causes a strong urge to scratch the skin, which can lead to lichenification with thickened and leathery skin [9,10]. This is among the possible complications of uncontrolled and persistent pruritus, which results in excoriation (scratching) and predisposes secondary bacterial infections. When pruritus is managed properly and treated, the risk of complications can be minimized and is instrumental in supporting better outcomes [6]. Traditional measures of pruritus are mainly grounded on clinical outcome assessments and patient-reported outcome assessments [11,12], which are subjective data and give little knowledge on symptom variation beyond clinical conditions. This may result in a misperception of the severity of the disease. Hence, additional indicators and objective measurements are required to assess the efficiency of treatment and underlying factors.

The development of wearable sensor devices has supported objective health measurements both in the outpatient and inpatient settings. Human scratching is commonly quantified by wrist-worn actigraphs, including ActiTrac and DigiTrac. In both cases, Ebata et al. and Hon et al. utilized accelerometers that can detect the movement in two and three axial planes, respectively [13–15]. But techniques based on accelerometer data find it difficult to accurately detect fine scratching motions constrained to fingers [16]. Alternatively, there are those approaches, where the sound of body-conducted scratching is detected, to document and measure the human scratching behavior, which is then usually followed by video recording [16–19]. This solution has the limitation of possible distraction by the surrounding sounds and is therefore not practical as a clinical solution, and difficult to automate [18]. A combination of inertial measurement unit and electric potential sensor data was suggested to measure scratching by Jocys et al. [20]. The deficiencies of this approach consist of the fact that several sensors should be attached to several body parts, which would, in practice, not be feasible. Other earlier applications, including Itchtector and Itch Tracker, use smartwatches and their acceleration sensors, demonstrating similar performance to actigraphy when detecting scratching actions [21,22]. But these applications will not differentiate arm and wrist movements.

In recent years, alternative methods to detect scratching with machine learning algorithms have been proposed [18–25]. Digital health technologies allow researchers to collect and analyze measurable data regarding many facets of health, including scratching behavior, which has already demonstrated good results. These technologies have the advantage of objective data capture [26]. As technology improves, there is a growing drive to invent new methods of detecting bio-signals, especially with new commercial wearables. Wearable medical technologies could transform healthcare by continuously monitoring. EMG is another of the most common biopotentials used with human-machine interfaces, through which muscle contractions can be measured by recording their electrical activity [27]. The movement in the forearm muscles can be monitored using this technique to determine scratching activity. The EMG analysis of the signals will help us to understand more about the muscle activity pattern related to scratching. This could be done by recording surface electromyography using a noninvasive method in order to ensure that the force of the contracting muscles beneath the skin is monitored [28].

The BIOPAC MP 36 is a well-known research-grade physiological signal acquisition system and has been extensively applied in biomedical research as it is highly reliable, precise, and applicable to an extensive array of biomedical signals. It is regarded as a gold standard system used in physiological signal acquisition due to the possibility of recording high-quality, reliable, and reproducible data on a variety of modalities, such as EMG, EOG, ECG, EEG, and EHG [35–39]. Its ability to record both low and high-frequency biomedical signals makes it essential to ensure that new biomedical devices and machine learning systems are validated. Its multi-channel recording capabilities, coupled with in-built noise reduction and ability to support sophisticated analysis

 doi:10.20944/preprints202604.1050.v1

software, make it reliable in characterizing the signals accurately, and provide a baseline upon which to compare wearable and experimental systems of acquisition. The BIOPAC MP 36 is significant because it is considered a reliable reference tool in research, and thus, the results of the experiment have standardized and clinically proven data, which increases the validity and generalizability of physiological data. Artificial intelligence algorithms can be used for the classification of scratch intensity [40]. A comparison between different modalities is represented in Table 1.

Table 1. Comparison Between Different Modalities to Detect Scratching.

Feature	EMG (Surface EMG)	Accelerometer (Actigraphy)	Acoustic (Sound)	Video/Camera
Data Source	Electrical activity of muscles (e.g., forearm).	Physical movement/acceleration of the limb.	Body-conducted sounds of scratching.	Visual recording of patient behavior.
Accuracy	High; detects fine motor activity and muscle synergy.	Moderate; struggles with fine finger movements.	Variable; can capture specific friction sounds.	High; but requires manual review.
Intensity Tracking	Able to classify Low, Medium, and High force.	Poor; often confuses general limb motion with scratching.	Limited data on force/pressure.	Subjective visual assessment of vigor.
Environmental Interference	Low; monitors signals beneath the skin.	High; movement from walking or arm waving creates noise.	High; easily distracted by surrounding ambient noise.	Lighting and occlusion can block view.
Feasibility	High, non-invasive and requires a wearable device.	High; usually integrated into a wearable device.	Low; requires sensors positioned to record body sound.	Low; privacy concerns and stationary setup.
Clinical Utility	Provides objective thresholds for skin damage.	Useful for general activity but lacks specificity for itch.	Difficult to automate and scale.	Mostly used to validate other sensors.

Hence, amongst physiological signals, EMG can be best suited for the detection of scratches and classification of their intensities with the help of machine learning models because it represents the electrical activity of muscles directly responsible for scratching. This paper examines how EMG signals can be analyzed and how machine learning can be used to automate the process of detecting scratching activity using sEMG signals recorded from extensor digitorum, flexor carpi radialis, and flexor digitorum superficialis muscles. A research-standard physiological signal acquisition system, BIOPAC MP 36, is used to acquire 3-channel EMG signals under a controlled paradigm. Using these signals, the movements of human muscles are studied to observe the differences in intensity. Also, the use of data collected across all three muscles enhanced the overall performance of the algorithm when tracking scratching behavior. Machine learning algorithms combined with EMG technology make it more effective to detect and analyze scratching behavior as well as to classify the scratch intensity as low, medium, and high. Irrespective of the advances made in the field of wearable actigraphy, there is still a considerable research gap: the failure to provide the objective definition of benign touch and the different levels of harmful scratching intensity. General limb motion is usually confused with localized scratching by indirect sensors. The present paper is the only pilot study to provide the first multi-muscle synergy estimate of scratch quantification. This will shift us away from motion-based detection and towards a more clinically relevant tool that will identify which force thresholds are clinically relevant when it comes to causing skin barrier degradation and subsequent lichenification.

2. Materials and Methods

2.1. Participants

The EMG signals were acquired from 50 right-handed healthy participants. The inclusion criteria required participants with no prior history of neurological, muscular, or dermatological conditions affecting skin sensitivity or muscle activity. This study was conducted in accordance with the Declaration of Helsinki and was also approved by the Ethical Review Board of Air University, Islamabad [29]. Before participating in the experiment, each participant was given a comprehensive verbal explanation of the paradigm and protocols involved, including the associated risks. Subsequently, each participant had signed an informed consent before proceeding with the experiment. The targeted age group was based on data from the National Health and Nutrition Examination Survey [2]. According to this, psoriasis and AD are more prevalent in individuals over the age of 20, with no difference in prevalence between men and women. Therefore, to ensure generalizability and comprehensive analysis, EMG was acquired from both genders. In total, 50 regional subjects, 25 males and 25 females, aged 18-27 years, were involved in the study. All the subjects were students and staff from Air University. Essential physiological parameters and patients' demographics were recorded before EMG acquisition and are documented in Table 2.

Table 2. Summary of participant demographics, physiological parameters, and database composition.

Parameter	Description
Age Group	22 ± 2.5
No. of participants	50
Oxygen Saturation	>94%
BMI	20-25
Dominant Hand	Right-handed
No. of channels	03
No. of repetitions	05
Scratching Intensities	Low, medium, high
Sampling rate (Hz)	2000

2.2. Experimental Paradigm

EMG represents the electrical activity of the muscles. The EMG indicates different signal patterns depending on the movement performed and the muscles used. The signal for itching is generated when sensory receptors in the skin detect an itch stimulus. These sensory signals are processed in the dorsal horn of the spinal cord and transmit the itching signal to the brain. The motor cortex and basal ganglia generate motor signals to produce scratching movements. These myoelectric signals, causing muscle contraction, controlled by the central nervous system, are recorded as an electrical signal in the form of EMG, as shown in Figure 1 (a). Thus, a complex motor response indicating the activation pattern of muscles is directly captured. This helps in recording the signal with higher specificity in detecting and distinguishing scratching intensity. A thorough study was conducted to identify the superficial forearm muscles responsible for scratching movements. The study showed that in total, there are seven primary muscles that directly contribute to finger movements of flexion and extension [30]. Out of these seven muscles, three superficial muscles were selected because of their signal quality and ease of access for sEMG electrode placement. The key muscles chosen were the extensor digitorum, flexor carpi radialis, and flexor digitorum superficialis muscles, as shown in Figure 1 (b). The electrode placement was made such that firstly the muscles are identified for each subject and the Ag/AgCl part of the electrode is exactly placed on the designated part of that muscle. For negative (white lead), it is placed on the belly of the muscle. For positive (red lead), it is placed on the insertion of the muscle. For ground (black lead), it is placed on the bony structure where there is no motion to avoid the motion artifact in the EMG signals. Hence, crosstalk amongst the muscles can be avoided effectively.

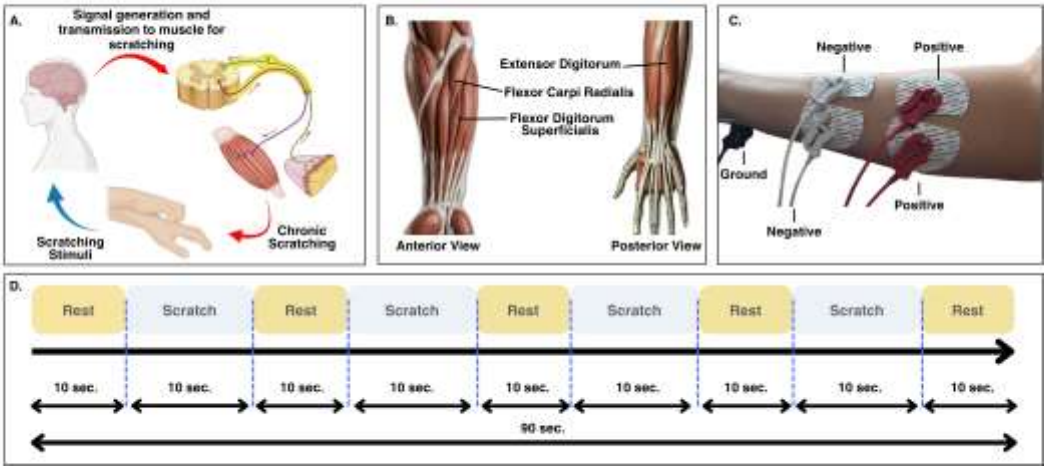

Figure 1. (a) EMG generation when scratching is initiated. (b) Illustration of the ventral (palmar) and dorsal aspects of the right forearm muscles. (c) Placement of recording electrodes to measure the scratching movement in the muscle. Two electrodes were placed longitudinally on each muscle to measure contractions of the extensor digitorum, flexor carpi radialis, and flexor digitorum superficialis. The electrodes with leads in red color are positive, in white color are negative, and in black are ground. (d) The resting phase shows no muscle activity, minimal muscle involvement is shown in low intensity scratching, moderate muscle activity is seen in medium intensity scratching, and high intensity scratching is indicated by a strong amplitude of the EMG signal. Varied EMG amplitudes are visible in dummy or non-scratching movements.

For each participant, the scratching activity of varying intensities was performed for five repetitions per intensity, with each intensity lasting 10 seconds, followed by 10 seconds of rest, as shown in Figure 1 (c). Verbal instructions were provided to prompt the initiation and cessation of the activity. To minimize signal interference, participants were instructed to maintain relaxed hand muscles throughout the recording session, as EMG signals may fluctuate with changes in hand orientation. Each participant was comfortably seated on a chair with a straight back and relaxed shoulders and arms. Prompts were provided to guide participants in increasing the scratching intensity using PsychoPy 2023.2.3 software. This helped the subject perform the activity according to the prompts displayed on the screen for a designated period. Data acquisition involved the recording of four distinct scratching motions: dummy, low intensity, medium intensity, and high intensity, along with that the fifth rest class as illustrated in Figure 2. The dummy scratching involved mimicking the action of scratching in the air. This is important for differentiating real and fake scratching in daily life, especially while the subject is sleeping. Hence, there are 5 different segments in the designed paradigm named as rest, dummy scratching, low intensity scratching, medium intensity scratching, and high intensity scratching. Using the PsychoPy 2023.2.3 software, during the low-intensity scratching, the subject was guided to scratch lightly, during the medium-intensity scratching, the subject was guided to scratch with moderate intensity, and finally, during high-intensity scratching, the subject was guided to scratch with high intensity. During all segments, the subject used the dominant right hand. This paradigm, with respect to time in seconds, was standardized for all 50 subjects, which means that the subject has to perform the required task within the assigned time.

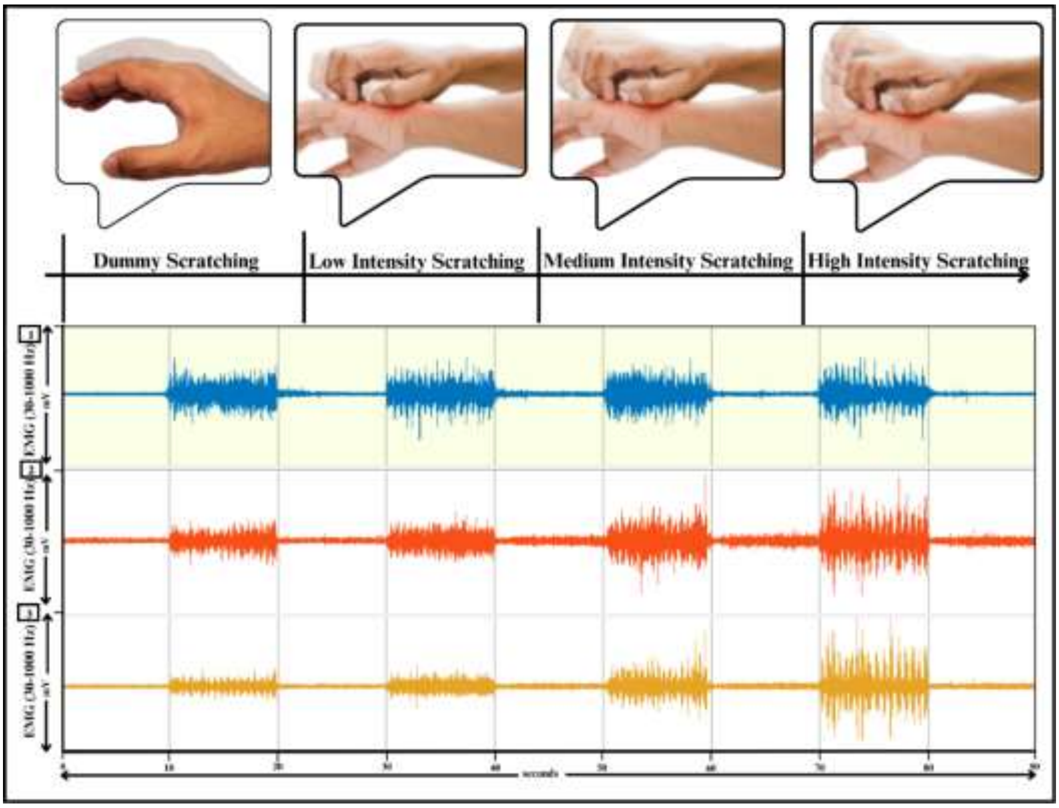

Figure 2. Paradigm for EMG Signal Acquisition: The paradigm includes five phases, i.e., Rest, Dummy Scratching, Low Intensity Scratching, Medium Intensity Scratching, and High Intensity Scratching.

To ensure robust data for machine learning based classification, five trials were performed for each movement for a duration of 90 seconds. After each trial, the participants were given a rest interval to minimize muscle fatigue. By adhering to this data collection protocol, a comprehensive dataset was compiled, representing the muscle activation patterns.

2.3. Experimental Setup

Preparatory measures were carried out before data acquisition for every participant. The subjects were asked to remove any jewelry or wristwatch they were wearing to acquire noise-free EMG. Before electrode placement, the skin was thoroughly cleaned using 70% isopropyl alcohol swabs to ensure optimal signal quality. The electrodes were then secured in place using adhesive tape to prevent any movement during data collection. For the acquisition of EMG signals, silver

doi:10.20944/preprints202604.1050.v1

chloride electrodes were strategically positioned on the forearm muscles shown in Figure 1 (b), targeting the extensor digitorum, flexor carpi radialis, and flexor digitorum superficialis muscles, while reference electrodes were affixed to both the wrist bones and the forehead. The electrodes are precisely adjusted in a manner to maximize the detection of signals from the desired muscle while minimizing the detection of signals from other muscles. The AgCl electrodes were used to minimize impedance and improve signal transmission. Figure 1 (c) shows the electrode placement on the right hand.

The BIOPAC MP 36 data acquisition system was used to acquire the desired EMG signals by utilizing its 3 channels. BIOPAC Systems, Inc., Goleta, CA, USA, is recognized for its advanced capabilities in real-time biological signal measurement and recording from the human body [31]. The acquired data were subsequently recorded by employing the AcqKnowledge software (BIOPAC Student Lab 4.1.1). The EMG signal was recorded at a sampling rate of 2 kHz (2000 samples per second) and then subjected to a filtering process. Initially, a 50 Hz notch filter was applied to eliminate power-line interference, followed by a band-pass Butterworth with lower and upper cut-off frequencies of 30 and 1000 Hz, respectively, to refine signal quality. The filters are predefined in BIOPAC Student Lab software with quality factor of 1. The amplitude of the sEMG signal is then recorded to analyze the intensity of the muscle activity engaged in a particular movement.

2.4. Feature Extraction

Raw EMG contains various noises and artifacts that cause decreased efficiency for classification. To enhance the classifier's performance, various EMG features were extracted to improve accuracy and effectiveness. This is achieved by transforming the input signal into a set of representative signal features, which enables the extraction of relevant information by filtering out unwanted components and interferences. The EMG feature sets are categorized into three main groups: time domain, frequency domain, and time-frequency or time-scale representation [32]. Despite the availability of multiple feature domains, time domain features are predominantly favored due to their superior classification performance and their lower computational cost compared to alternative domains. They offer an efficient approach to feature extraction, as they do not require additional transformations and are computed directly from raw EMG time series data [33]. In total, 10-time domain features were extracted, also targeting the Hudgins feature set [34]. The 3-channel EMG from Extensor Digitorum, Flexor Digitorum Superficialis, and Flexor Carpi Radialis muscles was used for processing and feature extraction. The features were extracted after EMG rectification and enveloping, as shown in Figure 3.

A total of 15 features were extracted from each channel of EMG, including both the time and frequency domain features. Hence, the total features for all 3 channels of EMG were 45. The features include mean, median, standard deviation, variance, covariance, kurtosis, skewness, root mean square, square integral, average energy, temporal moment, willison amplitude, zero crossing, mean frequency, and median frequency.

The features are described as,

Mean: It is the average amplitude of the EMG signal that shows the central tendency of muscle activity in the time domain. It also reflects the baseline level of muscle contraction. It can be represented by an equation as

$$\mu = \frac{1}{N}\sum x[n] \qquad (1)$$

Where μ is the mean value of the EMG signal, N is the total number of samples, and $x[n]$ is the amplitude of the EMG signal at the name n.

Median: It is the middle value of the EMG signal distribution. It is helpful in EMG analysis where sporadic spikes may appear.

$$Median(x) = middle\ value\ of\ sorted\ \ x[n] \qquad (2)$$

Where $Median$ is the middle value of the ordered EMG amplitudes and $x[n]$ is the amplitude of the EMG signal at sample n.

Standard Deviation: It is the variability of the EMG signal around the mean value. A high value of standard deviation indicates larger fluctuations in muscle activity. It can be represented by an equation as

$$\sigma = \sqrt{\left(\frac{1}{\mathrm{N}}\right)\sum (x[n] - \mu)^2} \quad (3)$$

Where σ is the standard deviation of the EMG signal, μ is the mean value of the signal, $x[n]$ is the amplitude of the EMG signal, and N is the number of samples.

Variance: It is the squared value of the deviation of the EMG signal from its mean value. It represents the muscle activation intensity.

$$\sigma^2 = \left(\frac{1}{\mathrm{N}}\right)\sum (x[n] - \mu)^2 \quad (4)$$

Where σ^2 is the variance of the EMG signal, μ is the mean value of the signal, $x[n]$ is the amplitude of the EMG signal, and N is the number of samples.

Covariance: It represents the similarity or dissimilarity of variance between two EMG signals. It is helpful in the quantification of muscle coordination.

$$Cov(X,Y) = \left(\frac{1}{\mathrm{N}}\right)\sum (x[n] - \mu_X)(y[n] - \mu_Y) \quad (5)$$

Where $Cov(X,Y)$ is the covariance between signals X and Y, μ_X is the mean value of signal X, and μ_Y is the mean value of signal Y, $x[n]$ and $y[n]$ are amplitudes of signals X and Y, and N is the total number of samples.

Kurtosis: It represents the peakedness of the amplitude of the EMG signal. A higher value of kurtosis shows a more frequent occurrence of extreme values.

$$Kurt(x) = \frac{\left(\frac{1}{\mathrm{N}}\right)\sum (x[n] - \mu)^4}{\sigma^4} \quad (6)$$

Where $Kurt(x)$ is the Kurtosis of the EMG signal, μ is the mean value of the signal, $x[n]$ is the amplitude of the EMG signal, σ is the standard deviation of the EMG signal, and N is the number of samples.

Skewness: It represents the asymmetry of the EMG signal distribution. It can be either positive or negative, depending on the patterns of the tail when plotted.

$$Skew(x) = \frac{\left(\frac{1}{\mathrm{N}}\right)\sum (x[n] - \mu)^3}{\sigma^3} \quad (7)$$

Where $Skew(x)$ is the Skewness of the EMG signal, μ is the mean value of the signal, $x[n]$ is the amplitude of the EMG signal, σ is the standard deviation of the EMG signal, and N is the number of samples.

Root Mean Square: It represents the effective value of the EMG signal, which corresponds to the energy of muscle contraction.

$$\mathrm{RMS} = \sqrt{\left(\frac{1}{\mathrm{N}}\right)\sum (x[n])^2} \quad (8)$$

Where RMS is the root mean square of the EMG signal, $x[n]$ is the amplitude of the EMG signal, and N is the number of samples.

Square Integral: It is the sum of squared amplitudes across the segment of an EMG signal. It represents a cumulative measure of the power of the EMG signal.

$$SI = \sum x[n]^2 \quad (9)$$

Where SI is the square integral of the EMG signal and $x[n]$ is the amplitude of the EMG signal.

Average Energy: It normalizes the power of the EMG signal per sample and provides a relative measure of activity intensity.

$$E_{avg} = \frac{1}{N}\sum x[n]^2 \quad (10)$$

Where E_{avg} is the average energy, $x[n]$ is the amplitude of the EMG signal, and N is the number of samples.

Temporal Moment: It shows the distribution of EMG signal energy with respect to time. Low values of temporal moment represent the mean and variance of the amplitude distribution, and high values represent the signal shape and temporal structure. It is important in identifying the muscle fatigue patterns.

$$M_m = \frac{1}{N}\sum (t_n - \mu_t)^{m\, x[n]} \quad (11)$$

Where M_m is the temporal moment of order m, t_n is the time index of the sample n, μ_t is the mean of time indices, $x[n]$ is the amplitude of the EMG signal, and N is the number of samples.

Willison Amplitude: It shows the number of times the absolute difference between the consecutive samples exceeds a predefined threshold. It is sensitive to changes in the muscle activity and reflects the complexity of the EMG signal.

$$WAMP = \sum f(|x[n+1] - x[n]| \geq \theta) \quad (12)$$

Where $WAMP$ is the Willison amplitude, $f()$ is the step function (1 if the condition is satisfied, else 0), θ is the threshold value, and $x[n]$ is the amplitude of the EMG signal.

Zero Crossing: It counts the number of times the EMG signal changes sign, representing the oscillatory activity within the muscle. It is also related to the dominant frequency content of the EMG signal.

$$ZC = \sum g(x[n], x[n+1]) \quad (13)$$

Where ZC is zero crossing count, $g(x[n], x[n+1])$ is the indicator function = 1 if sign change occurs, else 0.

Mean Frequency: It is the average frequency value of the EMG power spectrum. It is weighted by spectral amplitude and provides the information regarding the spectral centroid.

$$MNF = \frac{\sum f_k P_{fk}}{\sum P_{fk}} \quad (14)$$

Where MNF is the mean frequency, f_k is the frequency bin, and P_{fk} is the power spectral density at frequency f_k.

Median Frequency: It is the frequency that divides the power spectrum into two equal halves.

$$\sum P_{fk}, f \leq f_{med} = \frac{1}{2}\sum P_{fk} \quad (15)$$

Where f_{med} is the median frequency, P_f is the power spectral density, and the condition is that power below the median frequency = half of the total spectral power.

2.5. Feature Selection, Optimization, and Machine Learning Classification

The proposed methodology, as shown in Figure 3, also includes the optimization of features using Recursive Feature Elimination. It is a wrapper-type feature selection method. RFE operates by trying to find a subset of features beginning with all features in the training set and then trying to remove features until the required number is achieved. It does this by training the given machine learning algorithm, which is in the middle of the model, ranking features by importance, rejecting the least important features, and re-training the model. This step is continued until only a desired number of features is left. The primary logic is that the most relevant features will produce the largest effects on the target variable and will therefore be more helpful in predicting the target. In each iteration, it uses a model, typically a linear regression or support vector machine, to estimate the relative importance of each feature, and the features with the least importance are dropped.

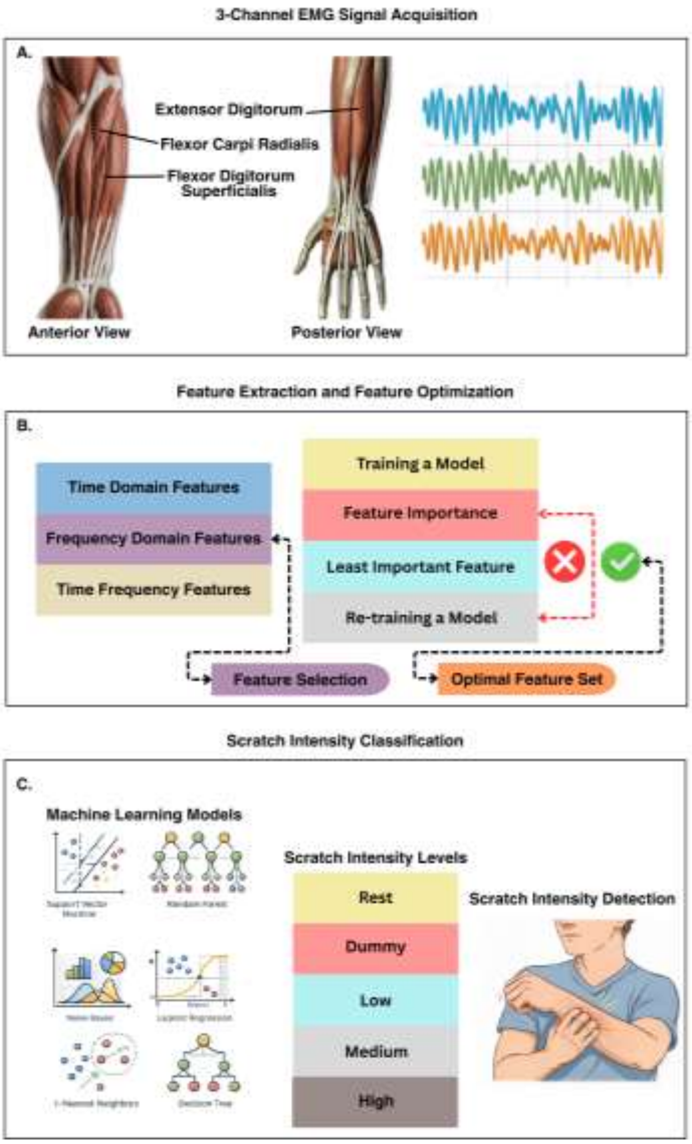

Figure 3. Overview of the proposed framework for scratch intensity detection using multi-channel EMG signals. (A) Placement of electrodes and acquisition of three-channel EMG signals from forearm muscles, including extensor digitorum, flexor carpi radialis, and flexor digitorum superficialis, along with representative signal waveforms. (B) Feature extraction (time-domain, frequency-domain, time–frequency, and nonlinear features) followed by recursive feature elimination (RFE), where features are iteratively ranked using model training and feature importance, least important features are removed, and the model is retrained to obtain an optimal feature subset. (C) Classification of scratch intensity using multiple machine learning models, categorizing activity into rest, dummy, low, medium, and high intensity levels for effective scratch behavior detection and prevention of lichenification.

Once the extracted features are optimized, they are used to train the machine learning classifiers for 5 different classes, i.e., rest, dummy scratch, low intensity scratch, medium intensity scratch, and high intensity scratch. The performance metrics are evaluated, including the test accuracy, precision, recall, F1 score, and 5-fold cross-validation accuracy. This process took a step-wise computational path in order to test and measure feature selection and classification of multi-channel EMG signal data. The dataset, in Excel format, was preprocessed first to locate the label and file names columns and deduce channel-based feature groups. To select features, a grid-search-based recursive feature elimination, combining with a Random Forest base estimator, was applied to all potential sizes of a feature subset, performing a stratified five-fold cross-validation. Random Forest has been used as the base estimator with recursive feature elimination (RFE) since it is suitable when working with data

 doi:10.20944/preprints202604.1050.v1

that is of high dimensionality and non-homogeneous, as in the case of multi-channel EMG signals in biomedical applications. Random Forest, being an ensemble learning algorithm that relies on bagging, decision trees, is useful at modeling complicated non-linear interactions between features and is also resistant to noise, variability, and overfitting, all of which are prevalent in EMG recordings. It provides an embedded feature ranking mechanism, which is based upon measures like Gini impurity reduction or permutation importance, and offers a statistically sound basis to iterative feature dropping in the RFE framework. In addition, Random Forest does not assume independent features and or a specific data distribution, and it is resistant to multicollinearity and scaling variance across time-domain, frequency-domain, and statistical EMG descriptors. This combination is what guarantees that the feature subsets that are chosen are discriminative and generalizable and have a higher reliability in future multi-classification of scratch intensities. The best subset of features in each channel arrangement (single, combined, and all channels) was selected according to the maximum cross-validation accuracy, and the chosen features were used in further modeling.

The configuration for Recursive Feature Elimination is represented in Table 3. Through the algorithm, a fixed random seed of 42 was set to ensure reproducibility. The extraction of features provided 45 features of three EMG channels including the time domain and frequency domain descriptors. Recursive Feature Elimination (RFE) was conducted based on a Random Forest classifier of 200 estimators and class balancing and was applied to 5-fold stratified cross-validation across all possible sizes of feature subsets. Multiplex machine learning models were utilized with default hyperparameters and their performance was measured both with stratified train-test splitting (80/20) and cross-validation. Oversampling, undersampling, SMOTE, ADASYN and SMOTE-ENN were used to deal with class imbalance. Standard scaling was used to normalize all features before the training of the models.

Table 3. Parameters in Recursive Feature Elimination Method.

Parameter	Value
Estimator	RandomForestClassifier
n_estimators	200
class_weight	balanced
Feature Selection	Exhaustive (1 to N)
Selection Criterion	Highest CV accuracy
Tie-break Rule	Smallest number of features

The classification phase used a wide variety of machine learning models, such as k-Nearest Neighbors, Linear Discriminant Analysis, Naive Bayes, Decision Tree, Random Forest, Support Vector Machine, Gradient Boosting, Multi-layer perceptrons, AdaBoost, Extra Trees, XGBoost, LightGBM, and CatBoost. In order to deal with possible class imbalance, various resampling methods were incorporated into the pipeline, such as random oversampling, random undersampling, SMOTE, ADASYN, and SMOTE-ENN, in addition to the original unbalanced data. All classifiers were trained and tested under these balancing plans on stratified five-fold cross-validation on training data, then independently tested on held-out test data. Accuracy, precision, recall, and F1-score were used as measures of performance, both as weighted averages and by class. The measure of overfitting was the difference between training and test accuracy. Classifier and balancing method comparisons were visualized using cross-validation curves, confusion matrices, and radar plots. Evidence-based interpretation of all intermediate and final results, such as selected features, classification metrics, and accuracy-overfitting summaries, was exported into formatted Excel files and graphical plots. This methodology allowed a strict comparison of feature selection strategies, balancing techniques, and classifiers to optimize the predictive performance in the provided dataset.

3. Results

Figures 4–6 shows the multichannel electromyography pattern of the muscles: Extensor Digitorum, Flexor Digitorum Superficialis, and Flexor Carpi Radialis during a controlled experimental paradigm consisting of five distinct conditions: rest, dummy scratch, low intensity scratch, medium intensity scratch, and high intensity scratch. The plots in the first row are time-domain EMG signals, the amplitude change in which distinctly indicates the intensity of various tasks; the more intense the task, the more intense the level of contraction and, accordingly, the more intense the EMG activity. The second row shows time-frequency analysis by the Short-Time Fourier Transform, which shows the nonstationary spectral variation of muscle activation. Distinct bursts of activity can be observed during the execution of tasks, especially when the intensity of the task is more demanding, with more robust motor unit recruitment. The frequency-domain representation, as represented by the Fast Fourier Transform, is presented in the third row and indicates the prevalent frequency content of muscle activity under the conditions. The fourth row shows the power spectral density as estimated by the Welch method, which provides a strong measure of the signal power distribution with respect to frequency bands. Taken together, these analyses offer a global description of EMG activity of the three muscles, both in terms of the temporal dynamics of the activity, spectral composition, and power distribution.

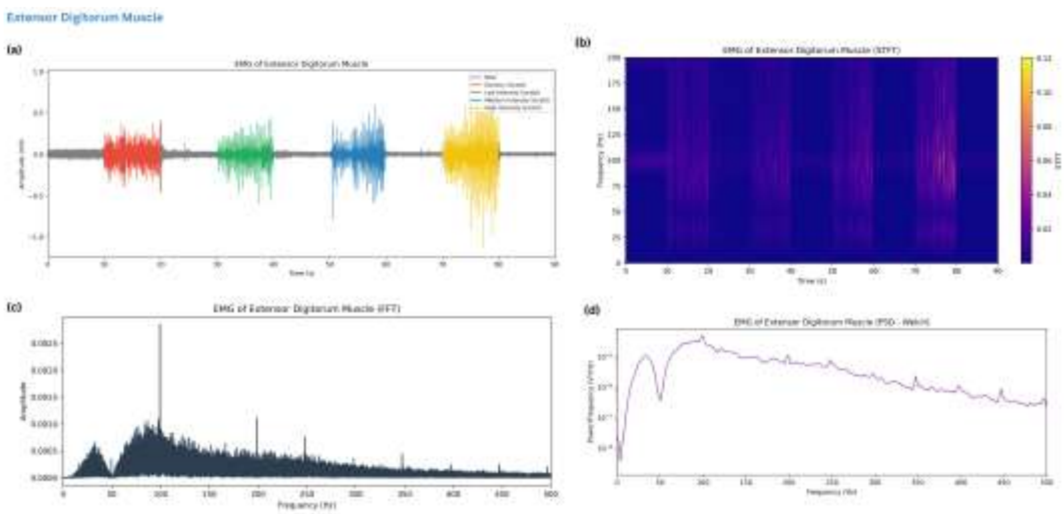

Figure 4. (a) EMG Acquired from Extensor Digitorum Muscle, (b) Short-Time Fourier Transform, (c) Fourier Transform, and (d) Power Density Spectrum of the Acquired 3-Channel EMG Signals according to the paradigm, including Rest, Dummy Scratch, Low Intensity Scratch, Medium Intensity Scratch, and High Intensity Scratch.

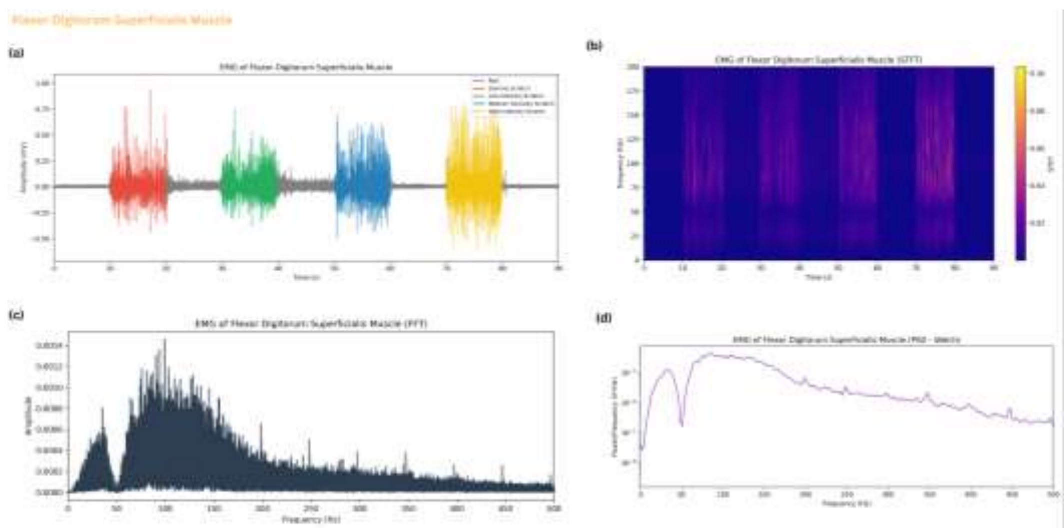

Figure 5. (a) EMG Acquired from Flexor Digitorum Superficialis Muscle, (b) Short-Time Fourier Transform, (c) Fourier Transform, and (d) Power Density Spectrum of the Acquired 3-Channel EMG Signals according to the paradigm, including Rest, Dummy Scratch, Low Intensity Scratch, Medium Intensity Scratch, and High Intensity Scratch.

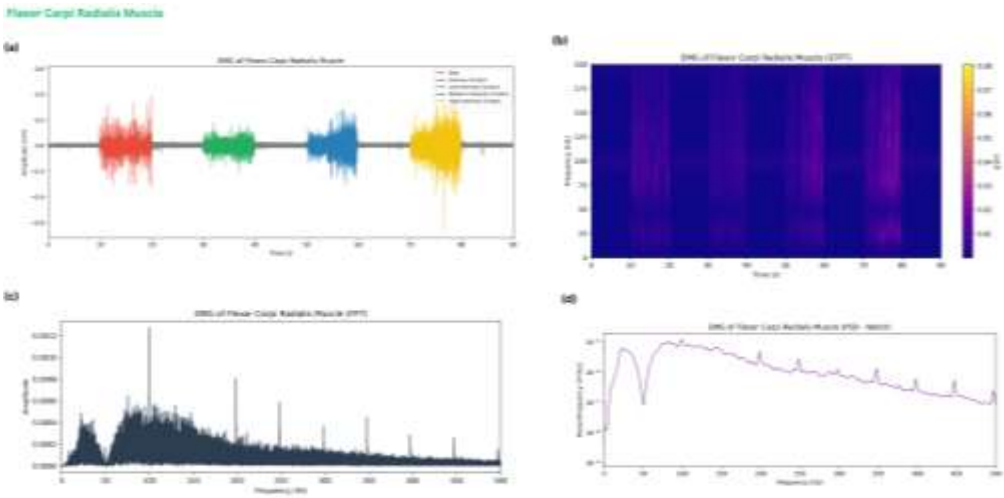

Figure 6. (a) EMG Acquired from Flexor Carpi Radialis Muscle, (b) Short-Time Fourier Transform, (c) Fourier Transform, and (d) Power Density Spectrum of the Acquired 3-Channel EMG Signals according to the paradigm, including Rest, Dummy Scratch, Low Intensity Scratch, Medium Intensity Scratch, and High Intensity Scratch.

Table 4 represent the impact of recursive feature elimination (RFE) on cross-validation accuracy when used on the original dataset with no augmentation, i.e., without using any conventional dataset balancing technique like random oversampling, random undersampling, synthetic minority over-sampling technique (SMOTE), adaptive synthetic sampling (ADASYN), and synthetic minority over-sampling edited nearest neighbor technique (SMOTE ENN). Classification accuracy increased with the number of features per muscle when the muscles were looked at separately, but then the performance leveled off. On the Extensor Digitorum muscle (CH1), twelve out of fifteen features were identified to be ideal, resulting in a cross-validation rate of 0.7429. In the case of the Flexor Digitorum Superficialis muscle (CH2), all fifteen features were selected, resulting in a maximum accuracy of 0.74, which indicates that the majority of the descriptors extracted on this muscle contained valuable information with minimum redundancy. The Flexor Carpi Radialis muscle (CH3) only needed ten features to achieve a maximum accuracy of 0.76, which shows that this muscle had a smaller set of discriminative features than the others. These results imply that the predictive ability of each channel is somewhat limited when channels are viewed individually. When the features of two muscles were optimized and combined, there was a noticeable improvement. The combination of Extensor Digitorum and Flexor Digitorum Superficialis muscles (CH1+CH2) accuracy was 0.8057 with twenty-nine features, whereas Extensor Digitorum and Flexor Carpi Radialis (CH1+CH3) accuracy was 0.8171 with twenty-seven features. The best accuracy between the two-muscle pairs was achieved in Flexor Digitorum Superficialis and Flexor Carpi Radialis (CH2+CH3), where the accuracy was 0.8229 and twenty-six features were selected. These findings show that the incorporation of complementary muscle information improves the discriminative power of the model because various muscles produce different activity patterns that represent more variability in the signal characteristics. It was also noted during feature selection that not every single descriptor was equally important, and in most instances, a smaller set of features was enough to give maximum accuracy. The above inclusion of the three muscles also enhanced the classification performance, with the maximum cross-validation accuracy of 0.8629 being obtained with forty-four features chosen among forty-five. The consistency in the improvement of the accuracy curve with the increase in the number of features, as well as the fact that almost the full set of features was kept, suggested that each channel of a given muscle contributed to information that was non-redundant and complementary. This confirms that multi-channel electromyography signals are synergistic muscle activations, and a combination of the signals is the strongest basis of classification. The chosen characteristics across channels were a combination of time-domain measures like standard deviation, variance, root mean square, and Willison amplitude, and frequency-domain measures like mean and median frequencies. Both temporal and spectral features are included in this modeling, which implies that differences in amplitude and frequency content play important roles in separating motor tasks. Interestingly, the Flexor Digitorum Superficialis muscle did not lose most of its characteristics, and its descriptors could have been quite informative, whereas the Flexor Carpi Radialis needed a smaller number of features to achieve the highest accuracy, which indicates its effectiveness in providing discriminative information. The Extensor Digitorum muscle displayed these two in balance, with a moderate number of features needed to generate maximum results. These results support the need to classify electromyography based on several muscle channels. Although single-channel analysis can be valuable, the combination of signals across many muscles can result in large improvements in accuracy because of the complementary nature of muscle activations. Recursive feature elimination was effective in finding the most relevant descriptors and reducing redundancy to make the classification model accurate and efficient. The results of high performance when the three muscles were applied jointly prove the importance of taking advantage of inter-muscular coordination patterns to achieve strong and stable motor task recognition.

Table 4. Channel-wise Feature Optimization using the Recursive Feature Elimination Method.

Muscle Name (s)	Channel (s)	No. of Total Features	No. of Features Selected	RFE Best CV Accuracy	Selected Features
Extensor Digitorum Muscle	CH1	15	12	0.742857	StdDev, Variance, Covariance, Kurtosis, Skewness RMS, Square Integral, Average Energy Temporal Moment, Willison Amplitude, Zero Crossing Mean Frequency
Flexor Digitorum Superficialis Muscle	CH2	15	15	0.74	Mean, Median, StdDev, Variance, Covariance Kurtosis, Skewness, RMS, Square Integral, Average Energy Temporal Moment, Willison Amplitude, Zero Crossing Mean Frequency, Median Frequency
Flexor Carpi Radialis Muscle	CH3	15	10	0.76	Median, StdDev, Variance, Covariance, Kurtosis, Skewness RMS, Square Integral, Average Energy Mean Frequency
Extensor Digitorum Muscle + Flexor Digitorum	CH1+ CH2	30	29	0.805714	CH1: Mean, Median, StdDev, Variance, Covariance, Kurtosis, Skewness, RMS, Square Integral, Average Energy, Temporal Moment, Willison Amplitude, Zero Crossing, Mean Frequency, Median Frequency CH2: Mean, Median, StdDev, Variance, Covariance, Kurtosis, Skewness, RMS, Square Integral, Average

Preprints.org (www.preprints.org) | NOT PEER-REVIEWED | Posted: 15 April 2026 doi:10.20944/preprints202604.1050.v1

Superficialis Muscle					Energy, Temporal Moment, Willison Amplitude, Zero Crossing, Mean Frequency
Extensor Digitorum Muscle + Flexor Carpi Radialis Muscle	CH1+CH3	30	27	0.817143	CH1: Median, StdDev, Variance, Covariance, Kurtosis, Skewness, RMS, Square Integral, Average Energy, Temporal Moment, Willison Amplitude, Zero Crossing, Mean Frequency CH3: Mean, Median, StdDev, Variance, Covariance, Kurtosis, Skewness, RMS, Square Integral, Average Energy, Temporal Moment, Willison Amplitude, Zero Crossing, Mean Frequency
Flexor Digitorum Superficialis Muscle + Flexor Carpi Radialis Muscle	CH2+CH3	30	26	0.822857	**CH2:** Mean, StdDev, Variance, Covariance, Kurtosis, Skewness, RMS, Square Integral, Average Energy, Temporal Moment, Willison Amplitude, Mean Frequency **CH3:** Mean, Median, StdDev, Variance, Covariance, Kurtosis, Skewness, RMS, Square Integral, Average Energy, Willison Amplitude, Zero Crossing, Mean Frequency, Median Frequency
Extensor Digitorum Muscle + Flexor Digitorum Superficialis Muscle + Flexor Carpi Radialis Muscle	ALL	45	44	0.862857	**CH1:** Mean, Median, StdDev, Variance, Covariance, Kurtosis, Skewness, RMS, Square Integral, Average Energy, Temporal Moment, Willison Amplitude, Zero Crossing, Mean Frequency, Median Frequency **CH2:** Mean, Median, StdDev, Variance, Covariance, Kurtosis, Skewness, RMS, Square Integral, Average Energy, Temporal Moment, Willison Amplitude, Zero Crossing, Mean Frequency **CH3:** Mean, Median, StdDev, Variance, Covariance, Kurtosis, Skewness, RMS, Square Integral, Average Energy, Temporal Moment, Willison Amplitude, Zero Crossing, Mean Frequency, Median Frequency

Recursive Feature Elimination (RFE) process only kept 44 out of 45 features in the final multi-channel model, indicating the high density of information and low level of redundancy of the extracted Electromyogram feature set. Instead of showing that there is a danger of overfitting, the fact that a wide range of features is retained indicates that each of the temporal and spectral elements of the neuromuscular synergy involved in scratching captures some different aspects of this phenomenon. Moreover, the consistency between the cross-validation performance (0.8629) and the independent test set performance is a powerful internal measure to overfitting, which verifies that the Machine Learning-based scratch detection model is effective at generalizing in the context of the synergistic activation patterns of the three forearm muscles.

The results from Figure 7 (a–d) and Figures in supplementary material show that balancing techniques can offer minor fine-tuning in certain machine learning classifiers. The multi-muscle feature space is rich and robust enough that most current classifiers can be trained to perform stably and well, even without extensive balancing. It suggests that the feature integration between the muscles is a more critical factor of the classification accuracy than the used balancing method. The spider plots when the features of individual muscles and combinations of them are used are provided in the supplementary material.

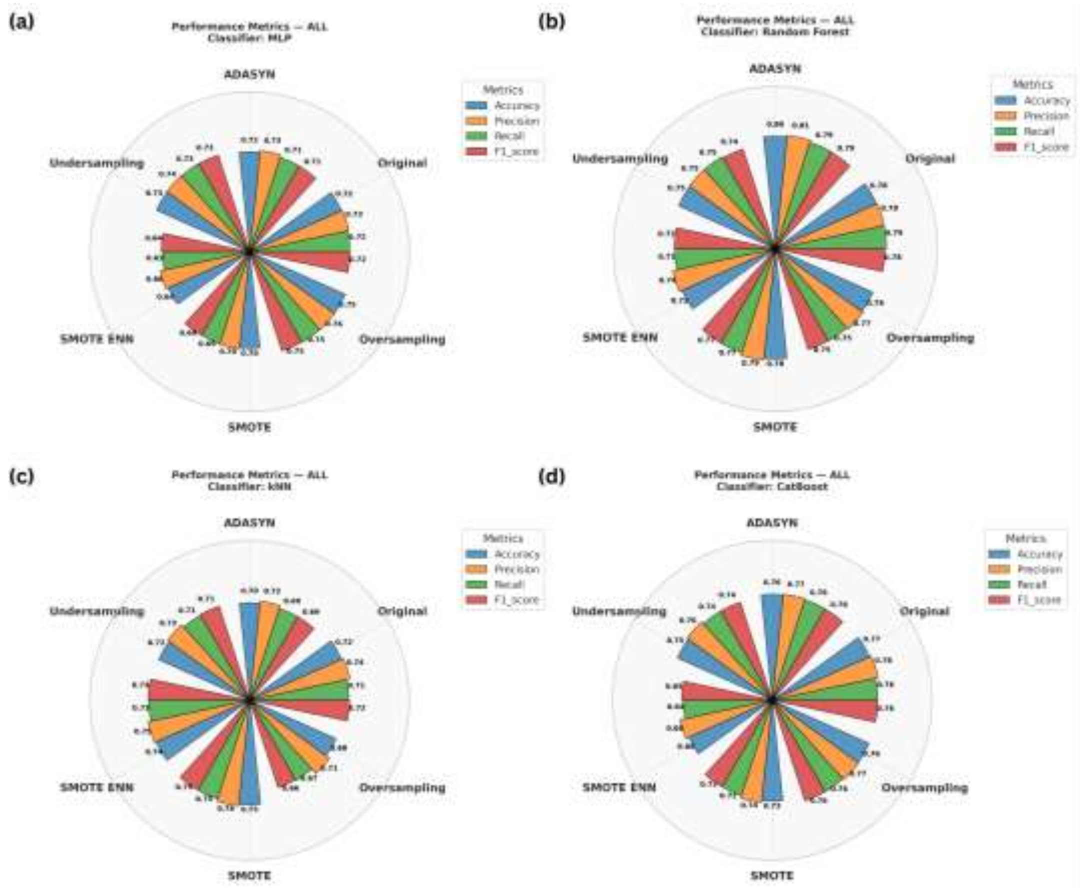

Figure 7. Radial Histogram Plots (a–d) representing performance metrics, i.e., Accuracy, Precision, Recall, and F-1 score for different machine learning classifiers, including features extracted from EMG of all three muscles, while different data balancing techniques are used.

Figure 8 (a–l) represents twelve confusion matrices, each corresponding to a different machine learning classification model applied to the original dataset without any balancing technique. The confusion matrices show how well each algorithm predicts categorical labels (Dummy, Low, Medium, High, Rest) compared to their true values.

Preprints.org (www.preprints.org) | NOT PEER-REVIEWED | Posted: 15 April 2026 doi:10.20944/preprints202604.1050.v1

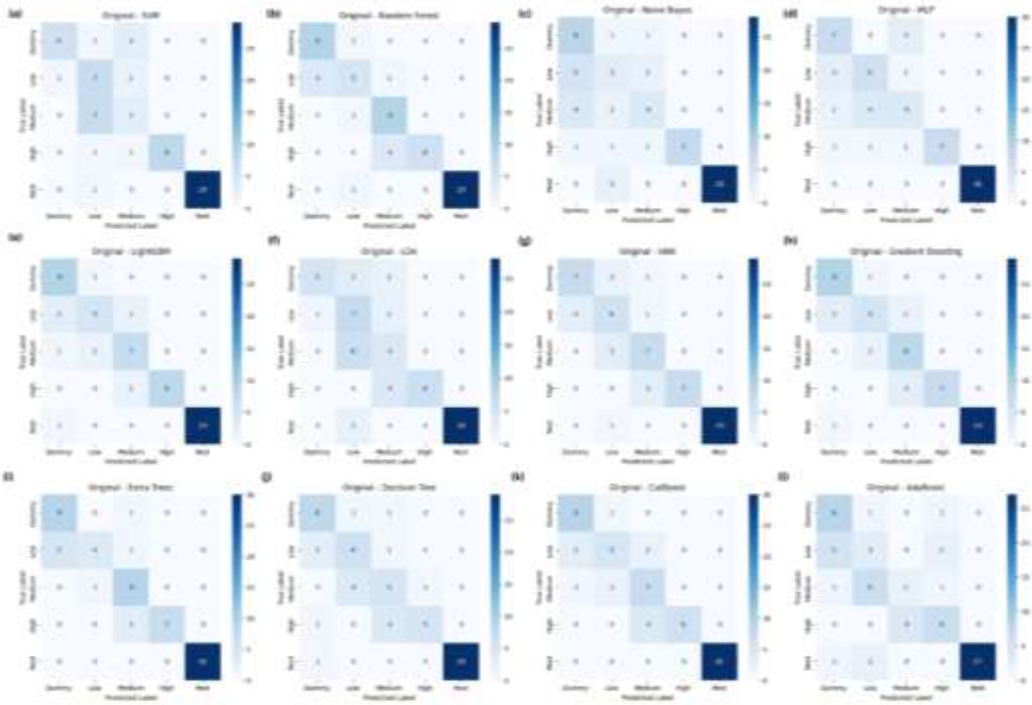

Figure 8. Confusion Matrices (a–l) Representing True and Predicted Labels when the original dataset is used without any balancing technique.

Table 5 shows that ensembles based on trees (Random Forest, Extra Trees, Gradient Boosting, LightGBM, CatBoost) are always balanced in terms of performance across classes. As an example, the maximum F1-scores of Dummy (0.82), Medium (0.72), and perfect Rest were created by Extra Trees. The performance of kNN and MLP also remains consistent, especially on Rest and High classes. Linear models (LDA, SVM, Naive Bayes) do reasonably well, separating well on Rest and High but with weaker performance in the Low/Medium locales, probably because the distributions of EMG features are nonlinear. The weakest in overall performance is AdaBoost, which does not perform well with Low and Medium intensities, suggesting that the complexity of the EMG data cannot be captured through boosting individual weak learners.

Table 5. Performance Metrics including Precision, Recall, and F-1 Score for individual classes when the original dataset is used without any balancing technique.

Classifier	Class	Precision	Recall	F-1 Score
k-Nearest Neighbours	Dummy	0.7	0.7	0.7
	Low	0.5	0.6	0.545455
	Medium	0.583333	0.7	0.636364
	High	1	0.7	0.823529
	Rest	1	0.966667	0.983051
Linear Discriminant Analysis	Dummy	0.833333	0.5	0.625
	Low	0.388889	0.7	0.5
	Medium	0.333333	0.4	0.363636
	High	1	0.6	0.75
	Rest	1	0.933333	0.965517
Naïve Bayes	Dummy	0.444444	0.8	0.571429
	Low	0.333333	0.3	0.315789

Preprints.org (www.preprints.org) | NOT PEER-REVIEWED | Posted: 15 April 2026 doi:10.20944/preprints202604.1050.v1

	Medium	0.5	0.4	0.444444
	High	1	0.7	0.823529
	Rest	1	0.933333	0.965517
Decision Tree	Dummy	0.666667	0.8	0.727273
	Low	0.461538	0.6	0.521739
	Medium	0.5	0.6	0.545455
	High	1	0.5	0.666667
	Rest	1	0.933333	0.965517
Random Forest	Dummy	0.666667	0.8	0.727273
	Low	0.571429	0.4	0.470588
	Medium	0.642857	0.9	0.75
	High	0.875	0.7	0.777778
	Rest	1	0.966667	0.983051
Support Vector Machine	Dummy	0.857143	0.6	0.705882
	Low	0.411765	0.7	0.518519
	Medium	0.333333	0.3	0.315789
	High	1	0.8	0.888889
	Rest	1	0.966667	0.983051
Gradient Boosting	Dummy	0.692308	0.9	0.782609
	Low	0.625	0.5	0.555556
	Medium	0.615385	0.8	0.695652
	High	1	0.7	0.823529
	Rest	1	0.966667	0.983051
Multilayer Perceptron	Dummy	0.636364	0.7	0.666667
	Low	0.461538	0.6	0.521739
	Medium	0.555556	0.5	0.526316
	High	1	0.7	0.823529
	Rest	1	1	1
AdaBoost	Dummy	0.533333	0.8	0.64
	Low	0.25	0.3	0.272727
	Medium	0.333333	0.2	0.25
	High	0.6	0.6	0.6
	Rest	1	0.9	0.947368
Extra Trees	Dummy	0.75	0.9	0.818182
	Low	0.8	0.4	0.533333
	Medium	0.6	0.9	0.72
	High	0.875	0.7	0.777778
	Rest	1	1	1
LightGBM	Dummy	0.642857	0.9	0.75
	Low	0.625	0.5	0.555556
	Medium	0.636364	0.7	0.666667
	High	1	0.8	0.888889

 doi:10.20944/preprints202604.1050.v1

	Rest	1	0.966667	0.983051
	Dummy	0.692308	0.9	0.782609
	Low	0.625	0.5	0.555556
CatBoost	Medium	0.538462	0.7	0.608696
	High	1	0.6	0.75
	Dummy	0.692308	0.9	0.782609

4. Discussion

This study provides evidence that surface electromyography is a valid and accurate modality to identify and measure scratching behavior, which is a major improvement over traditional devices like accelerometers, gyroscopes, video surveillance, or acoustic measurement. The electrical activity of extensor digitorum, flexor carpi radialis, and flexor digitorum superficialis could be recorded to capture neuromuscular activity directly related to scratching with a degree of precision unattainable by movement sensors or other indirect methods. The findings indicate that, whilst individual muscles yield informative patterns, multi-muscle recordings yield a richer feature space, which can be used to classify scratching with greater confidence across different intensities. This is a clear indication that the discriminative information necessary to be detected accurately is not carried in any isolated channels by the muscle, but rather in the synergistic activity of the muscles. The identified features in the optimized features section of this work were temporal descriptors of variance, root mean square, and Willison amplitude, and frequency-based descriptors of mean and median frequencies. The combination of time and frequency-domain features shows that the process of scratching cannot be characterized by amplitude variation or spectral changes alone, but by a combination of both. To overtly reduce the risk of overfitting, we used Stratified 5-Fold Cross-Validation with tree-based ensemble classifiers. The dataset is divided into five folds using this approach and preserves the original class distribution (Rest, Dummy, Low, Medium, High) in every fold. The model is trained and validated in four folds with the fifth fold, and this is repeated to expose the model to all the inter-subject variability in the Electromyogram signals. The stability of the high cross-validation value and the ultimate test accuracy confirm that the features which were retained are real neuromuscular patterns and not dataset peculiarity so that the efficacy of the proposed framework in the prevention of lichenification can be justified. The balance represents the physiological truth that scratching is composed of both sustained muscle contractions as well as dynamic oscillatory patterns, neither of which can be ignored to produce correct classification. Using recursive feature elimination, redundant information was eliminated and the most important features retained, enhancing interpretability and allowing the model to generalize to data outside the experimental data.

These results correspond with the earlier literature highlighting the constraints of using accelerometers and gyroscopes to detect fine-motor activities. These sensors tend to identify the slight movements of fingers as noise and result in a false negative in scratching. Likewise, acoustic techniques are susceptible to noise pollution by the surrounding atmosphere, and they are not specific enough to be used clinically. Video surveillance, as precise as it is, is very questionable in terms of privacy and feasibility, especially when it comes to living sub-units where round-the-clock observation is not a viable option. Conversely, the method described here is based on non-invasive EMG electrodes on the forearm, directly recording the motor codes of scratching. This offers sensitivity to fine activity as well as specificity to the scratching activity itself and renders the system more reliable and more adaptable to wearable use. The practical usefulness of EMG-sensing is that the pre-scratch, muscle tension can be observed and the precise amount of energy used in the act. SEMG offers high fidelity signature of skin trauma risk, as opposed to cameras that are constrained by the line of sight and privacy issues when used at night, or accelerometers, which do not differentiate between intensity in cases when the arm is at rest. This enables a Prevention-First paradigm in which haptic feedback may be activated whenever muscle activity during scratching is classified by machine learning algorithm. Future work will involve a clinical trial with dermatological

 doi:10.20944/preprints202604.1050.v1

patients to correlate EMG amplitude directly with Dermatologist-labeled Scratch Severity Scales and histological markers of skin thickening. Furthermore, the integration of a real-time haptic feedback loop will be tested to evaluate whether automated alerts can effectively disrupt the 'itch-scratch cycle' and prevent the onset of lichenification in naturalistic, nocturnal environments.

The current approach has very high performance using a simple three-channel setup, compared to earlier multimodal methods, which often involve the combination of many sensors located at various sites on the body. This simplification of hardware construction is more likely to be translated into a working device. Moreover, the machine learning pipeline used in this case outperforms the previous thresholding or rule-based approach, as it empirically optimizes the classification limits by prioritizing feature value. Of particular interest is the capacity to differentiate between dummy scratching, low intensity scratching, and higher intensity scratching, as such a level of granularity can give clinically relevant information regarding the severity of scratching that cannot be achieved using binary detection systems. The strengths of the study contribute to the work in the field in several ways. The direct EMG measurement methodology also means that the scratching is detected on the level of muscle activity, as opposed to secondary effect detection, so the system is very sensitive to even low-level activity. The interaction of three muscles is able to gather complementary information, and flexors and extensors are considered as complementary but synergistic patterns. The rich set of features provides the strength of considering both the time and spectral properties of the signals. Streamlining of feature optimization by recursive elimination optimizes the model, preserving accuracy, reducing computing load, and improving generalizability. Lastly, the work in this research is easily applicable to a future implementation in a portable or wearable device, which opens up real-time applications.

The limitations of the work should be considered as an opportunity to continue developing the work. It is a proof-of-concept study in which the EMG data of only healthy subjects is acquired under a controlled paradigm of self-induced scratching. It can be validated in the future on subjects with pathological scratching problems. The experiments were carried out in controlled laboratory conditions where data of high cleanliness was obtained without completely replicating the nature and everyday conditions. Although the scope of the subject group was restricted to healthy young adults, further application to other population groups, such as those with chronic pruritus or dermatological conditions, will offer the clinical validation required to ensure translation. Recording periods were relatively short and involved structured trials, whereas in the real world, long-term data acquisition would be necessary to capture spontaneous cases of scratching, including those that would occur during sleep. Also, the BIOPAC MP 36 acquisition system is operationally feasible, though additional development is required to downsize the hardware, minimize power usage, and provide fully wireless operation that can be worn. Such considerations lead to further directions that can develop the good results achieved here. Clinical validation in patients with chronic itch will determine the practical utility and aid in correlating the degree of scratching with the severity of the disease or response to the therapy. Patterns of scratching that cannot be observed during short controlled sessions will be identified through longitudinal monitoring in naturalistic settings (turned on overnight recordings). A reduction of the acquisition system into a wearable form factor, e.g., a smartwatch or an armband, will be more convenient and will increase patient compliance. Computationally, it can be enhanced with adaptive machine learning techniques or deep learning models to achieve a higher accuracy in the resulting classification and enable the system to adapt to the personal user over time. The itch scratch cycle and stress responses would be even better assessed with multimodal fusion with other physiological cues, including electrodermal activity or heart rate changes. In addition to monitoring, the system can be combined with therapeutic feedback loops, including haptic signals or electrical stimulation, to decrease scratching behavior and avoid skin damage.

This work provides a background to a paradigm shift in scratching detection. It is a viable and precise solution to continuous monitoring since it eliminates indirect and unreliable proxies and employs direct neuromuscular measurement. The possibility to not only detect but also measure the

 doi:10.20944/preprints202604.1050.v1

intensity of scratching offers new possibilities in clinical management of chronic pruritus, such as the objective evaluation of the activity of the treatment and the prevention of its complications, such as lichenification. As it advances and gains clinical validation, this method has significant potential to become a crucial instrument in both research and patient care, eventually leading to a better outcome and quality of life for patients with chronic itch.

5. Conclusions

Existing scratch detection devices are far capable of detecting complex hand movement and the intensity level associated with itching and scratching. An EMG signal contains important, useful information regarding the neuromuscular system that can be studied by analyzing these signals. This approach reduces the reliance on movement-based features, which makes it more effective in distinguishing the movement and the different scratch intensities. It also minimizes errors by eliminating the confounding factors like external body movements. In the future, clinical trials can be conducted for validation on subjects with scratching issues, and a therapeutic system can be integrated for prevention as well as treatment of lichenification.

Supplementary Materials: The following supporting information can be downloaded at the website of this paper posted on Preprints.org. The supplementary figures are provided for results section. .

Author Contributions: MOC: Conceptualization, Algorithm development, Feature optimization, Formal analysis, and Writing – original draft preparation. AA: Data collection, Data curation, and Validation. ZMUD: Methodology design, Signal preprocessing, and Supervision. JZG: Feature optimization, Project administration, Supervision, and Correspondence. AAA: Project administration and Supervision. HAG: Supervision.

Funding: The study was funded by the Deanship of Graduate Studies and Scientific Research at Qassim University QU-APC-2024-9/1.

Institutional Review Board Statement: The study was conducted in accordance with the Declaration of Helsinki, and approved by the Institutional Review Board of Air University (AU/EA/2023/606/18/2 and November 23, 2023).

Informed Consent Statement: Informed consent was obtained from all subjects involved in the study.

Data Availability Statement: The data supporting the findings of this study are not publicly available due to patient privacy and institutional restrictions. However, anonymized data and analysis scripts can be obtained from the corresponding author upon reasonable request.

Acknowledgments: The Researchers would like to thank the Deanship of Graduate Studies and Scientific Research at Qassim University for financial support [QU-APC-2024-9/1].

Conflicts of Interest: The authors declare no conflicts of interest.

References

1. Lavery, M.J.; et al. Nocturnal pruritus: Prevalence, characteristics, and impact on ItchyQoL in a chronic itch population. Acta Derm. Venereol. 2017, 97, 513–515.
2. Chen, W.; et al. Annoying Psoriasis and Atopic Dermatitis: A Narrative Review. 2022, 1–17.
3. Smith, M.P.; et al. Emerging methods to objectively assess pruritus in atopic dermatitis. Dermatol. Ther. 2019, 9, 407–420.
4. Raap, U.; Limberg, M.M.; Kridin, K.; Ludwig, R.J. Pruritus and increased risk of autoimmune skin blistering diseases: A propensity-matched global study. Biomolecules 2023, 13.
5. Ständer, S.; et al. Clinical classification of itch: Position paper of the International Forum for the Study of Itch. Acta Derm. Venereol. 2007, 87, 291–294.
6. Ju, T.; van der Does, A.V.A.N.; Mohsin, N.; Yosipovitch, G. Lichen Simplex Chronicus Itch: An update. Acta Derm. Venereol. 2022, 102, 1–6.
7. Gibson, M.C. Itch epidemiology and demographics. 2024. Available online: https://www.wikidoc.org

 doi:10.20944/preprints202604.1050.v1

8. (accessed 28 April 2024).
9. CDC. Skin Exposures and Effects. 2024. Available online: https://www.cdc.gov/niosh/topics/skin
10. (accessed 28 April 2024).
11. Price, A.; Cohen, D.E. Assessment of pruritus in psoriasis and atopic dermatitis: Subjective and objective tools. 2014, 25, 1–6.
12. Harris, A.C.T.B.B.W. Lichen Simplex Chronicus. 2023. Available online: https://www.ncbi.nlm.nih.gov/books/NBK499991
13. (accessed 2 April 2024).
14. Mahadevan, N.; et al. Development of digital measures for nighttime scratch and sleep using wrist-worn wearables. npj Digit. Med. 2021, 4, 1–10.
15. Elman, S.; Hynan, L.S.; Gabriel, V.; Mayo, M.J. The 5-D itch scale: A new measure of pruritus. Br. J. Dermatol. 2010, 162, 587–593.
16. Van de Water, A.T.M.; Holmes, A.; Hurley, D.A. Objective measurements of sleep outside laboratory settings: A systematic review. J. Sleep Res. 2011, 20, 183–200.
17. Ebata, T.; Iwasaki, S.; Kamide, R.; Niimura, M. Wrist activity monitoring for nocturnal scratching in atopic dermatitis. 2001, 305–309.
18. Hon, K.E.; et al. Measurement of pruritus in pemphigoid gestationis using a wrist movement detector. 2008, 64–67.
19. Noro, Y.; et al. Novel acoustic evaluation of scratching behavior in itching dermatitis. J. Dermatol. 2014, 41, 233–238.
20. Okuyama, T.; Hatakeyama, K.; Tanaka, M. Measurement of human scratch behavior using a compact microphone. Int. J. Appl. Electromagn. Mech. 2014, 45, 731–737.
21. Chun, K.S.; et al. A skin-conformable wireless sensor to objectively quantify pruritus symptoms. Sci. Adv. 2021, 7.
22. Yang, A.F.; Chun, K.S.; Patel, S.R. Performance metrics of a soft wearable acousto-mechanic sensor for measuring itch. Br. J. Dermatol. 2023, 188, 1.
23. Jocys, Z.; Pouryazdan, A.; Roggen, D. Multimodal fusion of IMUs and EPS sensors for scratch recognition. PervasiveHealth 2020, 325–335.
24. Lee, J.; et al. Itchtector: A wearable-based mobile system for managing itching. CHI Conf. Hum. Factors Comput. Syst. 2017, 893–905.
25. Ikoma, A.; et al. Measurement of nocturnal scratching using a smartwatch: Initial studies. Acta Derm. Venereol. 2019, 99, 268–273.
26. Stuntebeck, E.P.; Ii, J.S.D.; Abowd, G.D. HealthSense: Classification of health-related sensor data via user-assisted ML. Year N/A, 1–5.
27. Petersen, J.; Austin, D.; Sack, R.; Hayes, T.L. Actigraphy-based scratch detection using logistic regression. IEEE J. Biomed. Health Inform. 2013, 17, 277–283.
28. Wang, K. Detection of human scratching activity using deep learning models. 2023, 66–70.
29. Wang, W.K.; Cesnakova, L.; Goldsack, J.C.; Dunn, J. Digital measurement of scratching during sleep: Review. J. Med. Internet Res. 2023, 25, 1–17.
30. Esposito, D.; et al. Biosignal-based HMIs for assistance and rehab: A survey. Sensors 2021, 21, 1–43.
31. Botros, F.S.; Phinyomark, A.; Scheme, E.J. EMG-based gesture recognition: Shift from forearm to wrist? IEEE Trans. Ind. Inform. 2022, 18, 174–184.
32. WMA. Declaration of Helsinki—Ethical Principles for Human Research. 2025. Available online: https://www.wma.net
33. (accessed 10 February 2025).
34. Lieber, R.L.; Jacobson, M.D.; Fazeli, B.M.; Abrams, R.A.; Botte, M.J. Architecture of arm and forearm muscles for tendon transfer. J. Hand Surg. Am. 1992, 17, 787–798.
35. BIOPAC. EMG: Electromyography. 2025. Available online: https://www.biopac.com
36. (accessed 11 February 2025).
37. Phinyomark, A.; Phukpattaranont, P.; Limsakul, C. Feature reduction and selection for EMG classification. Expert Syst. Appl. 2012, 39, 7420–7431.

doi:10.20944/preprints202604.1050.v1

38. Bhattachargee, C.K.; Sikder, N.; Hasan, M.T.; Al Nahid, A. Finger movement classification using time–frequency EMG features. IC4ME2 2019, 11–12.
39. Chowdhury, R.H.; et al. Surface EMG signal processing and classification techniques. Sensors 2013, 13, 12431–12466.
40. Cheema, M.O.; Mohy-Ud-Din, Z.; Al Aishan, A.; Gul, J.Z. LaborEase: AI-based wearable EHG device for preterm detection. IEEE Access 2025, 13, 95457–95474.
41. Cheema, M.O.; et al. EOG-based physical stress detection. In Proceedings of the ICCDA, Oman, 2024; pp. 1–4.
42. Gul, J.Z.; Cheema, M.O.; Mohy Ud Din, Z.; Khan, M.; Kim, W.Y.; Rehman, M.M. ML-based classification of body imbalance using EMG and GRF. Appl. Sci. 2024, 14, 8209.
43. Gul, J.Z.; et al. Advanced sensing for sleep bruxism via EMG and ML. Sensors 2024, 24, 5426.
44. Ishtiaq, A.; Gul, J.; Mohy Ud Din, Z.; Imran, A.; El Hindi, K. Wearable AI-enabled bruxism detection. IEEE Access 2025, 13, 15503–15528.
45. Jafri, M.J.; Khan, F.S.; Ahmed, S.; Amjad, F. Scratch intensity classification with LSTM. In Proceedings of ICCDA, Oman, 2024; pp. 1–5.